

SUPPORTING INFORMATION

Impact of sodium hypochlorite on rejection of non-steroidal anti-inflammatory drugs by biomimetic forward osmosis membranes

Walid Ghamri^{1,2}, Patrick Loulergue¹, Irena Petrinic³, Claus Hélix-Nielsen^{3,4}, Maxime Pontié⁵,
Noureddine Nasrallah², Kamel Daoud², Anthony Szymczyk^{1*}

¹ *Univ Rennes, CNRS, ISCR – UMR 6226, F-35000 Rennes, France*

² *University of Science and Technology Houari Boumediene, Department of Mechanical and
Process Engineering, Algiers, Algeria*

³ *University of Maribor, Faculty of Chemistry and Chemical Engineering, Smetanova 17,
2000 Maribor, Slovenia*

⁴ *Department of Environmental Engineering, Technical University of Denmark,
Bygningstorvet 115, 2800, Kongens Lyngby, Denmark*

⁵ *Angers University, Group Analyses and Processes, Department of Chemistry, 2 Bd.
Lavoisier, F-49045 Angers 01, France*

*Corresponding author: anthony.szymczyk@univ-rennes1.fr

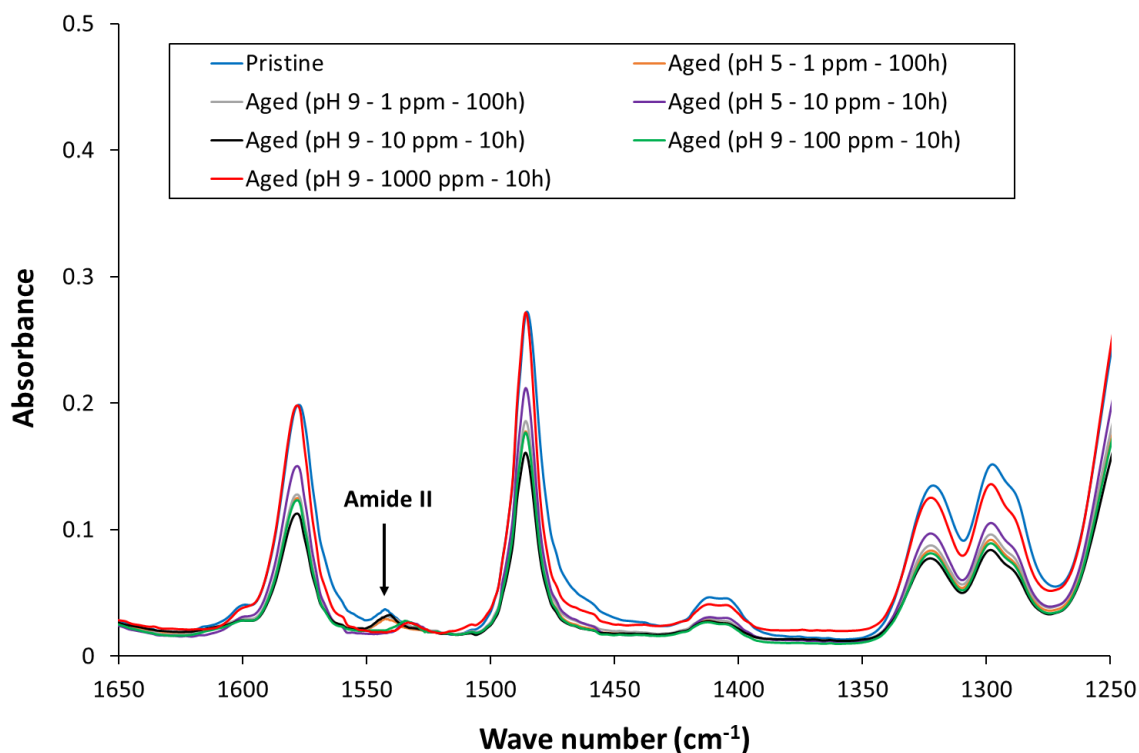


Figure S3. FTIR-ATR spectra of new and aged AQP membranes (active layer sides).

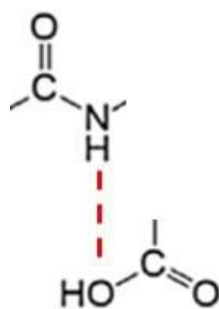


Figure S4. Hydrogen bond (red broken line) between the amidic hydrogen and the oxygen atom of the hydroxyl group of carboxylic acid.

When this hydrogen bond is broken due to N-chlorination of the amide group, the OH bond of the carboxylic acid group gets stronger, which makes it more difficult to deprotonate.

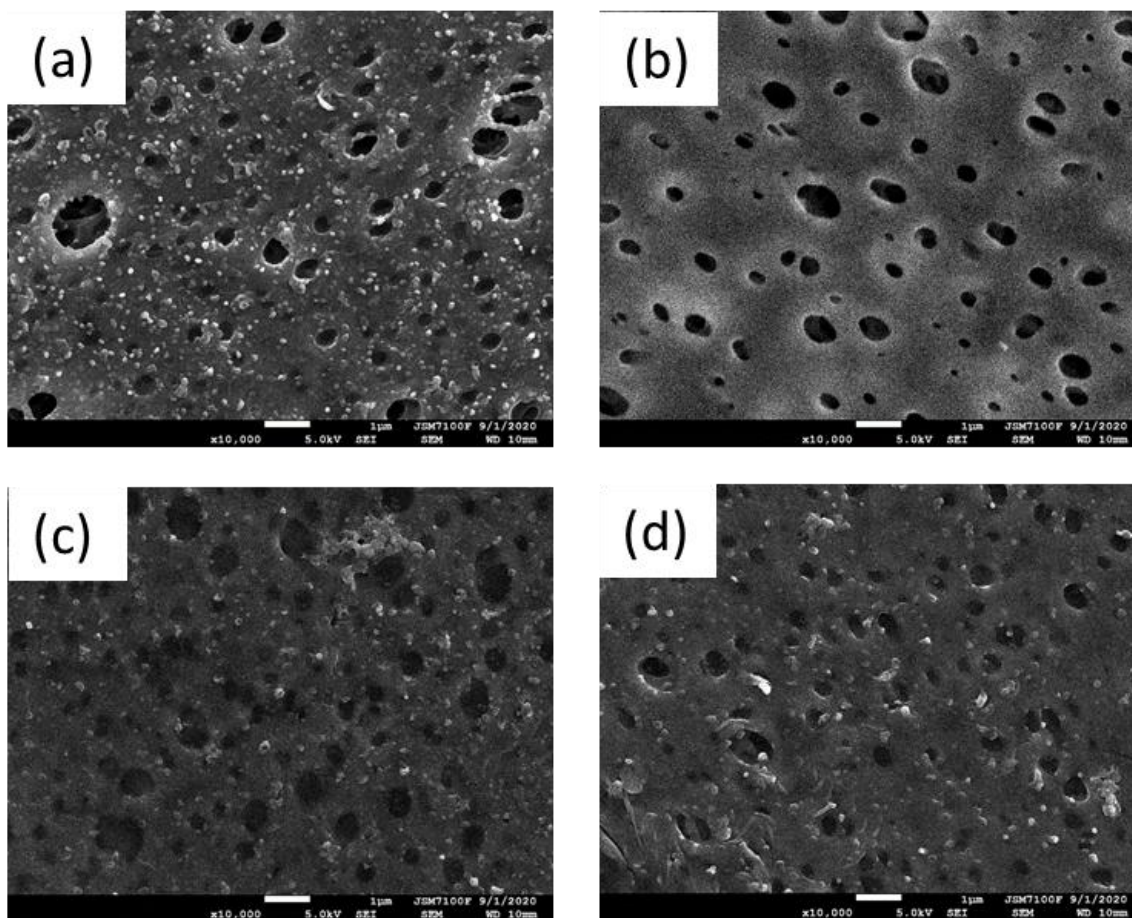


Figure S5. SEM images of AQP membrane surfaces. (a) Pristine membrane (active layer); (b) Pristine membrane (support layer); (c) Membrane aged in 10 ppm NaOCl at pH 9 for 10 h (active layer); (d) Membrane aged in 1000 ppm NaOCl at pH 9 for 10 h (active layer).

The surface morphology revealed by SEM was similar to that reported by Xia et al. for another aquaporin flat-sheet membrane for forward osmosis [2]. Polyamide nodules are visible on the images of the active layer of both the pristine and aged membranes (see Fig. S5 a, c and d). The porous structure of the support layer, with pore sizes in the range ~ 0.1 - $1 \mu\text{m}$ (see Fig. S5 b) can be seen even on the figures showing the active layer side of the membranes. Of course, this cannot be attributed to defects in the membrane active layers as all the membranes were found to exhibit very high naproxen and diclofenac rejections (around 98 %). This is most likely the result of damage to the thin active layers caused by the high vacuum during the sample preparation.

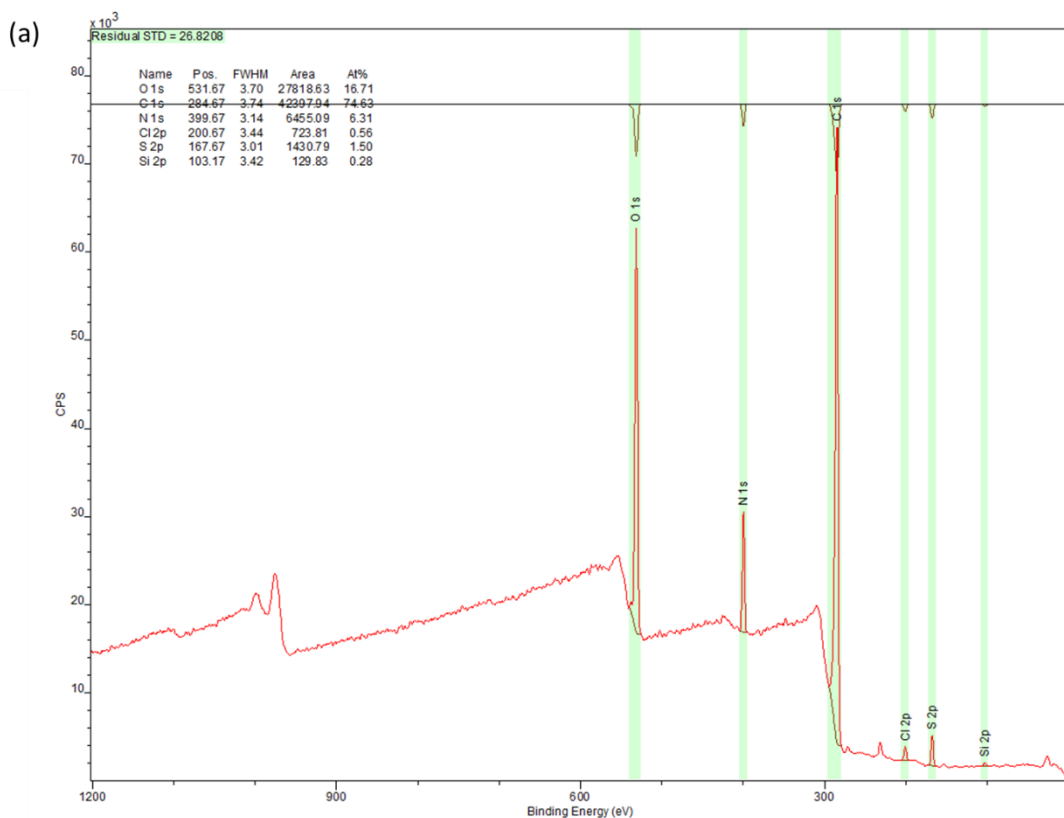


Figure S6. XPS wide spectrum of the AQP membrane active layer after ageing in 1000 ppm NaOCl at pH 9 for 10 h.

The detection of sulfur (coming from the PES support) indicates that the active layer was damaged during the sample preparation (most likely by the high vacuum). Chlorine was detected as a result of N-chlorination after exposure to sodium hypochlorite.

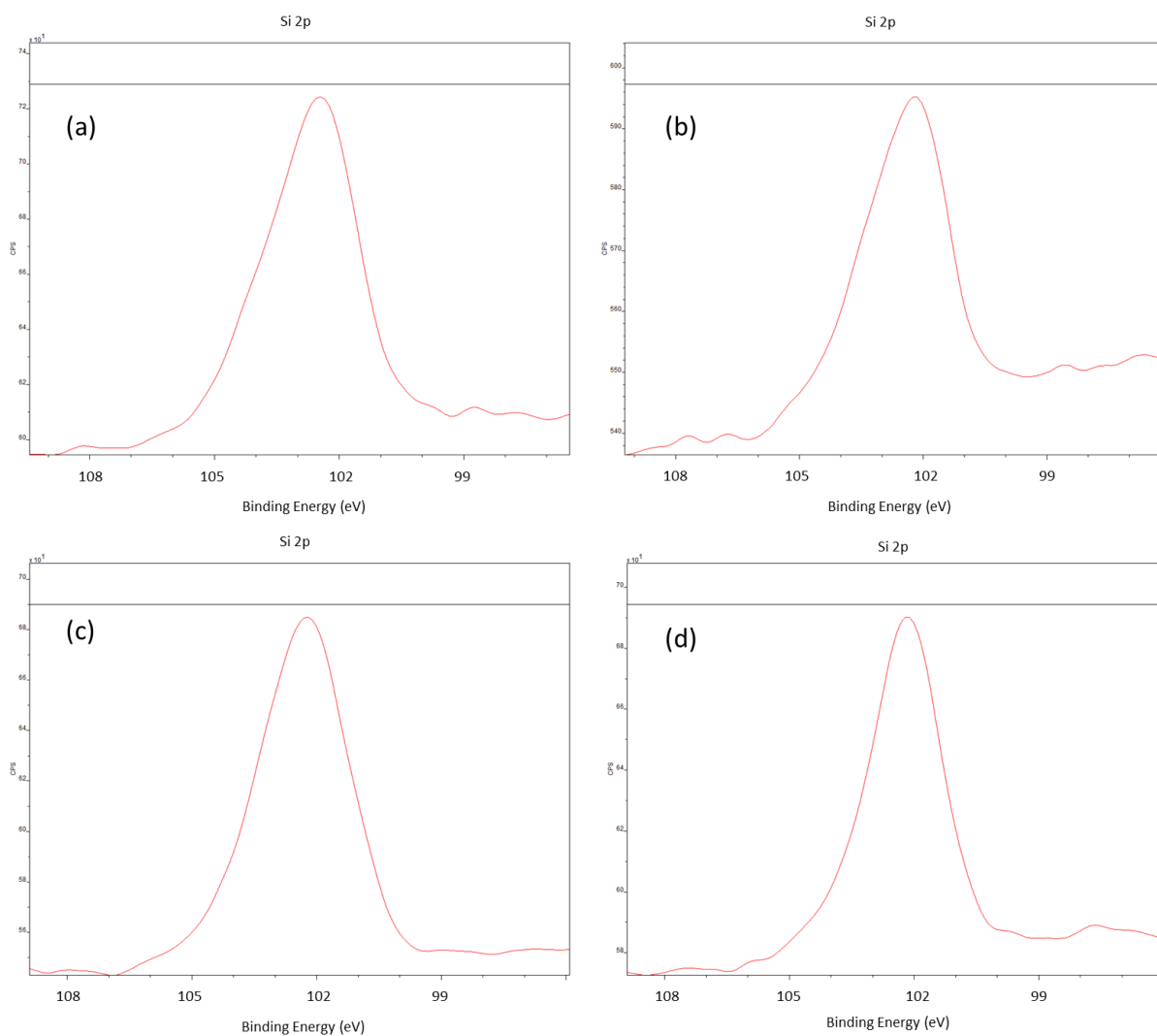
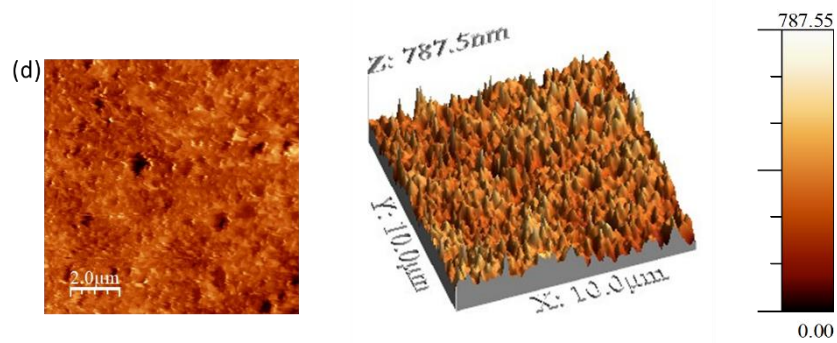
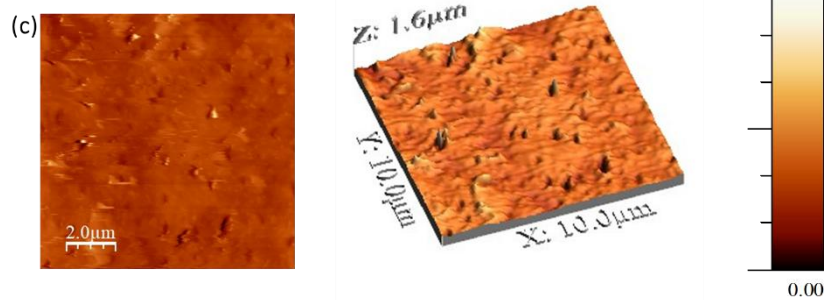
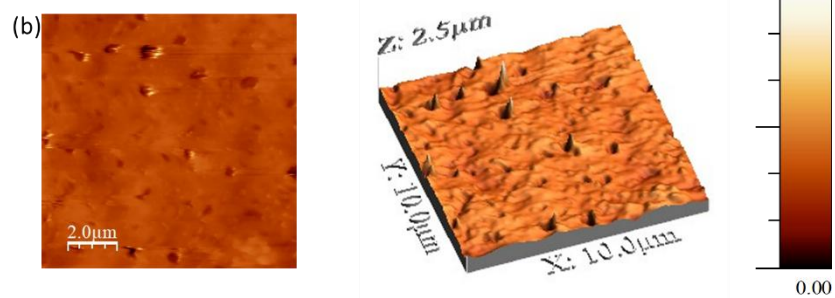
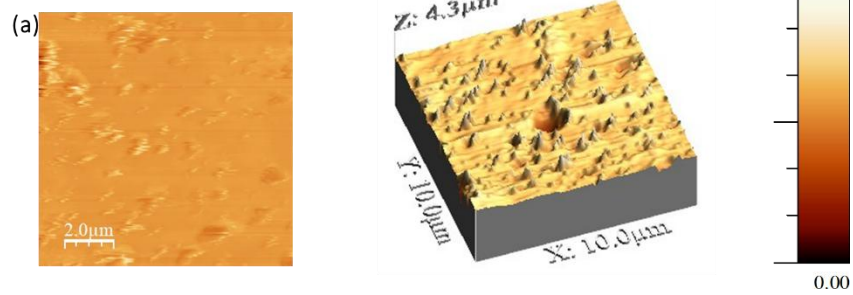


Figure S7. Si 2p XPS spectra of AQP membrane active layers. (a) pristine membrane; (b) membrane aged in 1 ppm NaOCl at pH 9 for 100 h; (c) membrane aged in 100 ppm NaOCl at pH 9 for 10 h; (d) membrane aged in 1000 ppm NaOCl at pH 9 for 10 h.

The presence of polymersomes incorporating aquaporins was confirmed by the detection of silicon (Si) on the surface of the various membranes (pristine and aged).



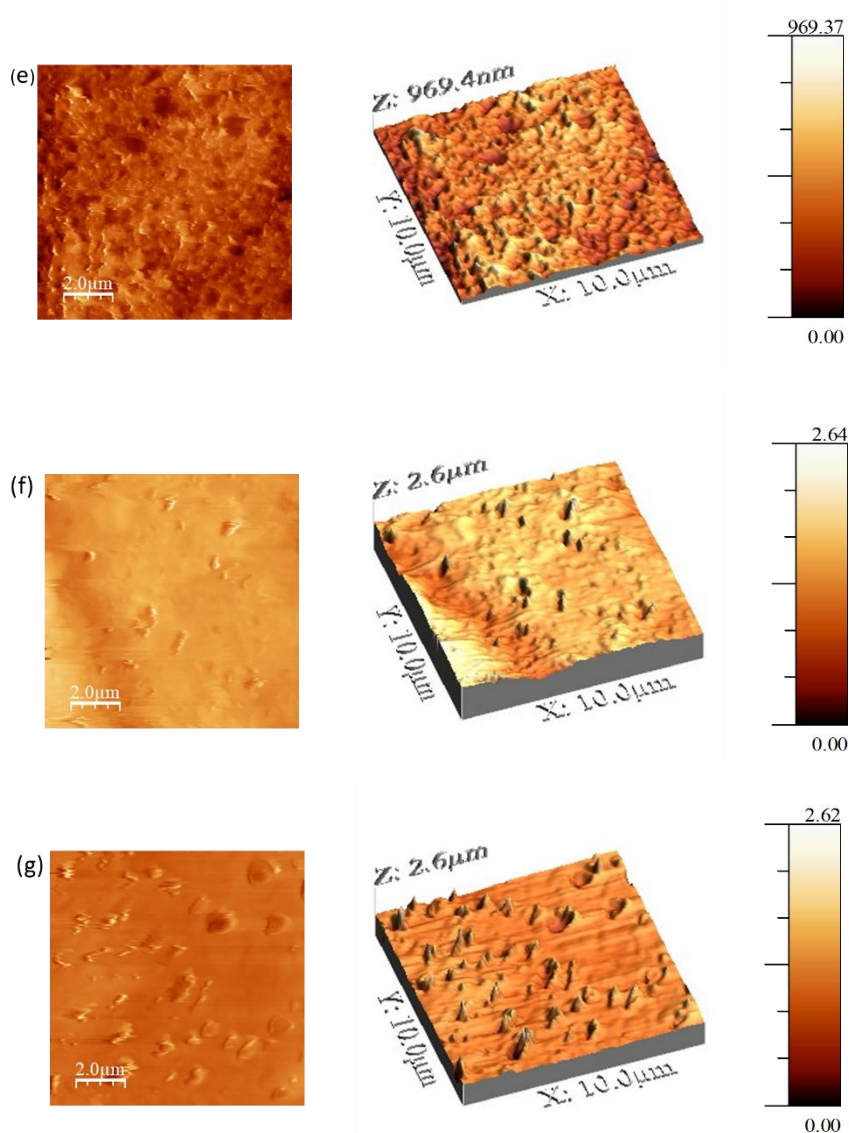


Figure S8. 2D and 3D AFM images of AQP membrane active layers. (a) pristine membrane; (b) membrane aged in 1 ppm NaOCl at pH 5 for 100 h; (c) membrane aged in 10 ppm NaOCl at pH 5 for 10 h; (d) membrane aged in 1 ppm NaOCl at pH 9 for 100 h; (e) membrane aged in 10 ppm NaOCl at pH 9 for 10 h; (f) membrane aged in 100 ppm NaOCl at pH 9 for 10 h; (g) membrane aged in 1000 ppm NaOCl at pH 9 for 10 h.

References

- [1] R. Verbeke, V. Gómez, I.F.J. Vankelecom, Chlorine-resistance of reverse osmosis (RO) polyamide membranes, *Prog. Polym. Sci.* 72 (2017) 1–15.
<https://doi.org/10.1016/j.progpolymsci.2017.05.003>.
- [2] L. Xia, M.F. Andersen, C. Hélix-Nielsen, J.R. McCutcheon, Novel Commercial Aquaporin Flat-Sheet Membrane for Forward Osmosis, *Ind. Eng. Chem. Res.* 56 (2017) 11919–11925.
<https://doi.org/10.1021/acs.iecr.7b02368>.